An MRI-compatible, Ultra-thin, Flexible Stimulator Array for Functional Neuroimaging by Direct Stimulation of the Rat Brain

Dongmin Kim, Yo Chin, Amir Reuveny, Tsuyoshi Sekitani, Takao Someya, *Member*, *IEEE*, and Masaki Sekino, *Member*, *IEEE*

***Abstract*—We developed an MRI-compatible, ultra-thin, flexible stimulator array for the rat brain and performed functional MRI (fMRI) acquisition during direct electrical stimulation of the brain. This technique measured brain activity evoked by direct stimulation of the motor and the somatosensory cortex. In order to avoid MR signal loss due to interferences with the main static field and RF field in the MRI system, the stimulator array was made from a non-magnetic gold electrode of 100-nm thickness on a 2-μm-thick parylene substrate. By using this stimulator array, MR images without signal loss around conducting electrode pads were acquired, and fMRI acquisition during concurrent electrical stimulation of the cerebral cortex was achieved. Neuronal activity propagated to distant brain areas from the stimulated motor cortex. Positive blood oxygenation level dependent (BOLD) signals were observed with direct stimulation of the motor cortex, while negative BOLD signals were observed with direct stimulation of the somatosensory cortex. Interestingly, the pattern of brain activity evoked by direct stimulation of the somatosensory cortex was different from that evoked by electrical stimulation of the forepaw.**

I. Introduction

Brain stimulation has been used as treatment for many neurological and psychiatric diseases, and this treatment is effective even in drug-resistant cases. Tsubokawa *et al*. first applied this treatment to patients with thalamic pain using implantable electrodes in the cerebral cortex [1]. They reported that direct stimulation of the motor cortex was effective for pain relief. Repetitive transcranial magnetic stimulation (rTMS) has recently been introduced as a non-invasive treatment for relieving neuropathic pain [2] [3]. These recent clinical studies report that stimulation of the motor cortex is effective in relieving pain, whereas stimulation of the somatosensory cortex is ineffective. In order to understand the mechanism of pain perception and the therapeutic effect of brain stimulation, studies using functional magnetic resonance imaging (fMRI) and positron emission tomography (PET) have been performed in both animals and humans [4]-[6]. Although fMRI has higher spatial resolution than PET, PET is advantageous for investigating brain activity evoked by electric stimulation due to the difficulty of fMRI acquisition of subjects with implanted electrodes [6]. This problem is caused by the interference of implanted electrodes with the static magnetic field and RF field in the MRI system.

To avoid degradation of magnetic resonance (MR) signals due to implanted electrodes, some recent studies have been performed by fabricating an MRI-compatible electrode with carbon fiber [7] or contriving the acquisition position using platinum–iridium wires [8]. Using these electrodes, brain connectivity from the cortex and modulated brain activity with deep brain stimulation were studied. However, coverage of multiple cortical areas is required for investigating the effect of stimulation of different target brain areas, and MRI-compatible electrodes for stimulating brain surface over large brain areas are not available.

In this study, we developed an MRI-compatible, ultra-thin, flexible stimulator array for direct brain stimulation covering the somatosensory and the motor cortex in the rat. Using this stimulator array, we evaluated MRI-compatibility by investigating attenuation of the MR signal intensity. In addition, we investigated brain activities at the areas of thalamus and insula related to pain processing [6] by directly stimulating the motor and the somatosensory cortex with a stimulation intensity of 80% of the motor threshold (MT) intensity.

II. Stimulator Array

A. MRI-compatibility

To avoid signal loss and degradation in MR images resulting from magnetic susceptibility effects, conducting parts and substrate of the stimulator array have to be fabricated with non-magnetic materials. Moreover, a shielding effect to RF pulse may cause degradation of images around conductive parts like electrode pads. To reduce the magnetic susceptibility effect and the RF attenuation, we fabricated the stimulator array by using only non-magnetic materials with ultra-thin gold electrode pads of 100-nm thickness on 1-μm-thick parylene substrate. Figure 1 illustrates RF wave propagation though a conducting medium with a thickness of t. In a conducting medium, the incident wave is attenuated and the attenuation constant α is given by

$$\alpha = \sqrt{\pi f \mu_0 \sigma} \quad (\mathrm{NP/m}) \tag{1}$$

where μ_0 is the permeability of free space, f is the frequency of incident electromagnetic wave, and σ is the conductivity of medium [9].

D. Kim, C. Yo, A. Reuveny, T. Sekitani, T. Someya, and M. Sekino are with the Department of Electrical Engineering and Information Systems, Graduate School of Engineering, the University of Tokyo, Tokyo 113-8656, Japan (e-mail: dongmin@bee.t.u-tokyo.ac.jp; chin@bee.t.u-tokyo.ac.jp; amir@ntech.t.u-tokyo.ac.jp; someya@ee.t.u-tokyo.ac.jp; sekino@bee.t.u-tokyo.ac.jp). And D. Kim, A. Reuveny, T. Sekitani, T. Someya, and M. Sekino are also with the Exploratory Research for Advanced Technology (ERATO), Japan Science and Technology Agency (JST), Tokyo 113-0032, Japan.

978-1-4244-7929-0/14/$26.00 ©2014 IEEE

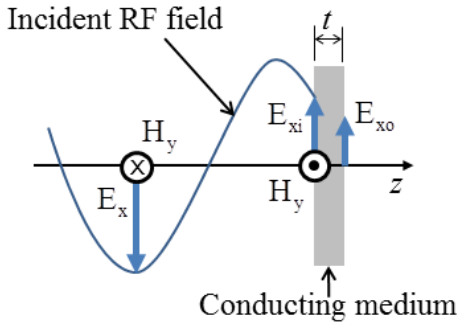

Figure 1. Propagation of electromagnetic waves through a conducting medium with thickness of *t*. Ex and Hy are the electric and the magnetic fields of the propagating electromagnetic wave. E_{xi} is the electric field induced by the incident wave and E_{x0} is the electric field at the distance of *t* from that.

Skin depth δ_s is given by

$$\delta_s = \frac{1}{\alpha} = \frac{1}{\sqrt{\pi f \mu_0 \sigma}} \quad (\mathrm{m}). \tag{2}$$

MRI-compatibility of the fabricated stimulator array can be evaluated by characterizing the amount of penetration an electromagnetic wave into a conducting medium using the attenuation constant and ratio to the skin depth.

B. Fabrication of Stimulator Array

Figure 2 shows a representation of the fabricated stimulator array. The parylene substrate was prepared with a thickness of 1 μm by chemical vapor deposition (CVD) on a silicon wafer. The pads and wires were fabricated by evaporating ~100 nm gold through a shadow mask on the parylene substrate. The location of the stimulating pads was determined according to the brain functional map [10] to match the motor and somatosensory cortex of the forepaw. An additional parylene layer of 1-μm thickness was deposited for encapsulation with masking the electrode pads and soldering pad. Prior to implantation, the stimulator array was peeled off from the silicon wafer to obtain ultra-thin, flexible electrode arrays.

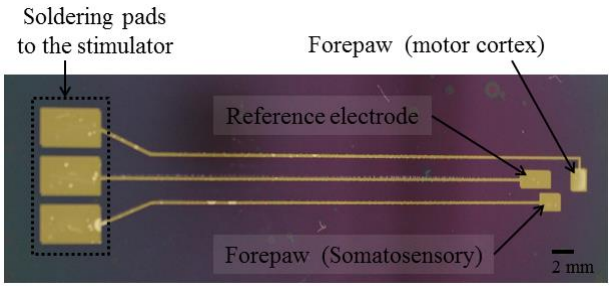

Figure 2. The MRI-compatible, ultra-thin, flexible stimulator array

III. Animal Experiments

All procedures were conducted in accordance with the University of Tokyo's guidelines regarding animal research and approved by the Ethics Committee of the university.

A. Implantation of Stimulator Array

Normal healthy male Wistar rats(240-260g;n=3) were used. The animals were individually housed in cages with food and water provided *ad libitum* and the room temperature was maintained at 18-20°C. The animals were anesthetized with 2-2.5% isoflurane mixed with air and placed in a stereotaxic frame to implant stimulator array. The temperature of the animal was maintained at 37°C using a rectal thermostat probe and a heating pad. The scalp was removed to expose the cranium, and the cranial bone was scraped and peeled off in an area of 7 × 3 mm^2 above the motor and somatosensory cortices of forepaw at the right hemisphere, as shown in Fig 3. The stimulator array was placed epidurally along the surface of the brain and fixed in place using biocompatible glue temporally. Using an acrylic resin, the stimulator array was fixed and insulated over the exposed skull area. An adhesive wide electrode (25 × 45 mm^2; V-040M4, NIHON KOHDEN Co.) was attached on the back at 30 mm from the head. A tail vein catheter was inserted to enable intravenous administration of the α-chloralose (Wako, Japan). Following surgery, α-chloralose (60 mg · kg^{-1}) was injected. Isoflurane administration was reduced to 1% and stopped after 5 minutes. After placing the animal in MRI system, the arousal level of anesthesia was confirmed by corneal reflex and hind limb withdrawal reflex. Once these reflexes were observed, the α-chloralose (10 mg · kg^{-1}· hr^{-1}) was administrated throughout MRI acquisition to maintain the arousal level of anesthesia.

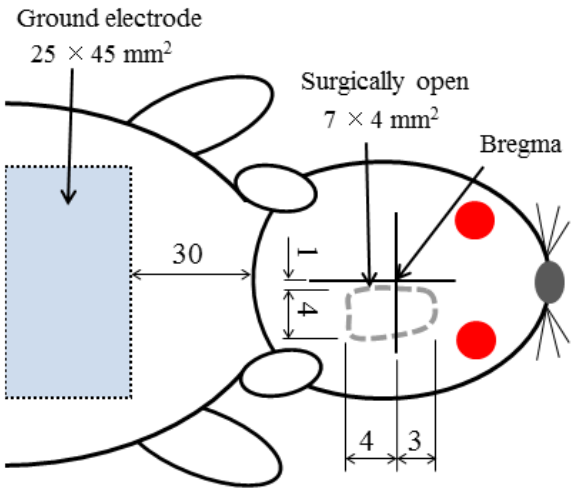

Figure 3. Implantation of the simulator array on the motor and the somatosensory cortex of the rat brain

B. Stimulus Conditions

Prior to direct brain stimulation, The MT current intensity was investigated by stimulating brain directly with square-wave pulse having width of 300 μs at the frequency of 3Hz [11]. When the contralateral forepaw began to move, it was determined. Stimulation of the motor and the somatosensory cortex was applied at 80% of the MT current intensity during fMRI acquisition. This level of stimulation intensity is used in clinical treatment for pain relief [12]. In the forepaw stimulation condition, electrical stimulation with the frequency of 3Hz, the pulse width of 300μs, and the current

intensity of 0.8 mA was delivered to the left forepaw of rat during fMRI acquisition.

C. Functional and Anatomical MRI Scans

MR images were acquired using a 7-T MRI system (BioSpec 70/20 USR, Bruker Co.). A FLASH pilot image was taken and the slice positions of the fMRI acquisition were determined. T2-weighted anatomical images were acquired using a RARE sequence with the following parameters: TR = 2500 ms, TE = 33 ms, FOV = 3 × 3 cm^2, matrix = 256 × 256, and slice thickness = 2 mm. For functional scans, gradient echo EPI sequence was used with TR = 1000 ms, TE = 13 ms, FOV = 3 × 3 cm^2, matrix = 64 × 64, and slice thickness = 2 mm. Ten coronal slices were acquired from 7 mm anterior to –15 mm posterior to the bregma. Functional MRI data was acquired with block design for 130 s during one brain stimulation trial consists of 60-second OFF, 30-second ON, and 60-second OFF. An inter-trial interval of 3 minutes was followed.

D. Data Processing and Analysis

Functional MRI data analysis was performed using an originally developed program. Brain area was extracted from images using a threshold method with maximum and minimum values of MR signal intensities that were determined manually on each averaged slice images. The time-series fMRI data was linearly correlated. Spatial smoothing was performed using a 2D Gaussian filtering method with Gaussian function of FWHM = 930 μm in all fMRI data to reduce noise. Statistical analysis was performed using Student's t-test, and differences were deemed to be statistically significant if $P < 0.01$. In order to identify the activated brain area, we merged the brain functional map of [13] to the averaged fMRI image with referring to the anatomical image.

IV. Result and Discussion

A. Evaluation of MRI-Compatibility

The magnetic resonance frequency and resulting RF frequency in 7-T MRI system are 300 MHz. Assuming the conductivity of gold to be 4.1 × 10^7 S/m, the attenuation constant α of the RF field is 2.2 × 10^5. The ratio of the attenuated electric field intensity with varying the thickness of the conducting medium calculated using equation (1) as shown in Fig. 4. The deduced skin depth on the gold electrode pad was 4.5 μm, as calculated by equation (2). The electrode pads of stimulator array was fabricated with a thickness of 100 nm. This electrode thickness is 1/750 to the bare electrode diameter used for fMRI scan with deep brain stimulation of [8] and 1/45 to the skin depth of gold medium. The electric field intensity can be calculated to be attenuated by 2.2 % of the incident RF field intensity through the gold electrode pad.

Figure 5 (a) shows the coronal image of the rat brain after implanting the stimulator array. Even though the RF coil for MRI acquisition was placed on the implanted area, neither artefacts nor signal loss were observed. Figure 5 (b) shows an oblique image that was acquired along the surface of the rat brain. Blood vessels on the cortex were clearly observed in the

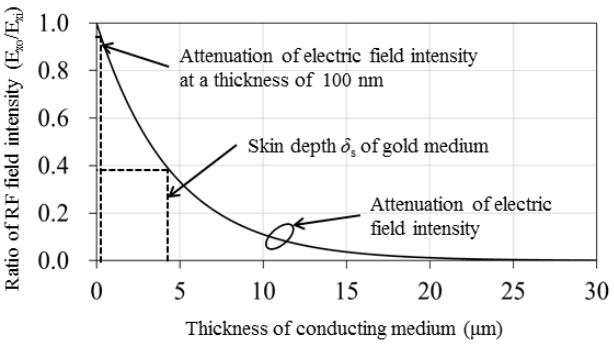

Figure 4. Attenuation of electric field intensity with the thickness of conducting gold medium

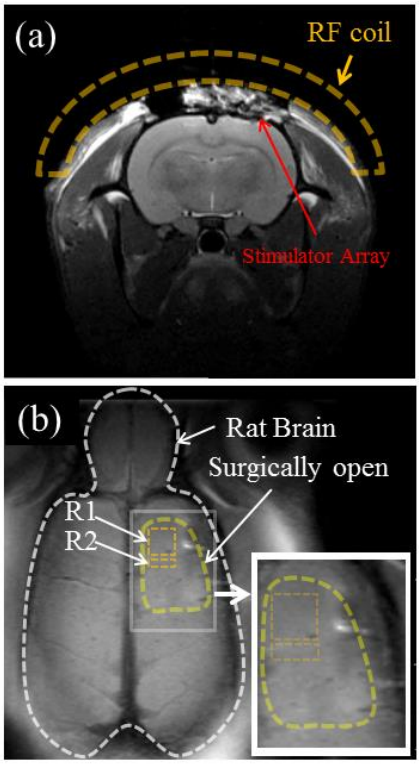

Figure 5. T2-weighted MR images with implanted stimulator array. (a) A coronal image of the rat brain. (b) An oblique image along the surface of the rat brain.

areas where the electrode pads were placed. The mean and standard deviation of MR signal intensity in the areas of R1 and R2 are shown in table 1. The area R1 includes the electrode pad. The area R2 includes parylene substrate but not the electrode pad. The MR signal intensity on the area R1 decreased by only 4.8 % to the area R2. The measured attenuation of MR signal intensity on the gold electrode pad was very close to the theoretically calculated attenuation level. This indicates the fabricated stimulator array has very good MRI-compatibility.

TABLE I. Distribution of MR Signal Intensity on The Location of Implated Stimulator Array

Area	Mean	Standard deviation
R1	7.29×10^5	3.92×10^4
R2	7.66×10^5	3.05×10^4

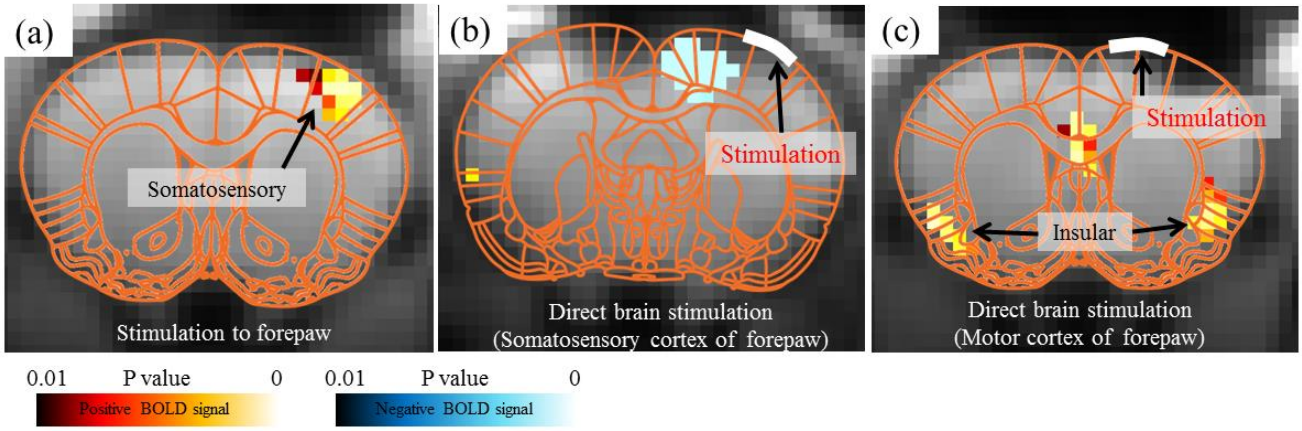

Figure 6. Mapping of Brain activation (a) Brain activation evoked by electrical stimulation of the rat forepaw. (b) Brain activation by direct stimulation of the somatosensory cortex of the forepaw. (c) Brain activation by direct stimulation of the motor cortex of the forepaw.

B. Brain Activation by Cortical Stimulation

Figure 6 shows a P value map with red and blue shades representing increment and decrement of blood oxygenation level dependent (BOLD) signals, respectively. The MT current intensities were 1.2-1.8 mA, and the impedances between the stimulation electrode and the ground electrode were 40-180 kΩ. As shown in Fig. 6 (a), electrical stimulation of the forepaw induced brain activation in the somatosensory cortex. However, in the direct stimulation condition of the somatosensory cortex, a negative BOLD signal was observed around the stimulated area as shown in Fig. 6 (b) and it might be followed by inhibiting the stimulation-evoked activations. In the direct stimulation condition of the motor cortex, brain activation around stimulated area was not observed, but distant brain areas of insular and thalamus was activated as shown in Fig. 6 (c). The thalamus relays somatosensory signals from periphery to the cortex and thalamus activation has been suggested to be necessary for pain relief [6]. These results complement that the activation of thalamus and insula is strongly involved in the treatment of neuropathic pain with direct electrical stimulation of the motor cortex.

V. Conclusion

In this study, we developed an MRI-compatible, ultra-thin, flexible stimulator array for the rat brain, and performed fMRI acquisition during direct electrical stimulation of the motor and somatosensory cortex. We observed negative BOLD signals following direct stimulation of the somatosensory cortex, in contrast to brain activation by the stimulation of the rat forepaw. We showed that brain areas of insula and thalamus distant from the stimulated region were activated in the direct stimulation of the motor cortex.

References

[1] T. Tsubokawa, Y. Katayama, T. Yamamoto, T. Hirayama, and S. Koyama, "Chronic motor cortex stimulation in patients with thalamic pain.", Journal of neurosurgery, vol. 78, no. 3, pp.393-401.

[2] J. P. Lefaucheur, X. Drouot, I. Ménard-Lefaucheur, Y. Keravel and, J. P. Nguyen, "Motor cortex rTMS restores defective intracortical inhibition in chronic neuropathic pain.", *Neurology*, vol. 67, no. 9, pp.1568-1574, 2006

[3] J. P. Lefaucheur, "The use of repetitive transcranial magnetic stimulation (rTMS) in chronic neuropathic pain.", *Neurophysiologie Clinique/Clinical Neurophysiology,* vol. 36, no. 3, pp. 17-124, 2006

[4] R. Peyron, B. Laurent, and L. Garcia-Larrea, "Functional imaging of brain responses to pain. A review and meta-analysis (2000).", *Neurophysiologie Clinique/Clinical Neurophysiology*, vol.30, no. 5, pp.263-288, 2000

[5] R. Peyron, M. Frot, F. Schneider, L. Garcia-Larrea, P. Mertens, F.G. Barral, M. Sindou, B. Laurent, and F. Mauguière, "Role of operculoinsular cortices in human pain processing: converging evidence from PET, fMRI, dipole modeling, and intracerebral recordings of evoked potentials.", *Neuroimage*, vol.17, no. 3, pp. 1336-1346, 2002

[6] L. García-Larrea, R. Peyron, P. Mertens, M.C. Gregoire, F. Lavenne, D. Le Bars, P. Convers, F. Mauguière, M. Sindou, and B. Laurent, "Electrical stimulation of motor cortex for pain control: a combined PET-scan and electrophysiological study.", *Pain*, vol.83, no. 2, pp.259-273, 1999

[7] V. C. Austin, A. M. Blamire, S. M. Grieve, M. J. O'Neill, P. Styles, P. M. Matthews, and N. R. Sibson, "Differences in the BOLD fMRI response to direct and indirect cortical stimulation in the rat.", *Magnetic resonance in medicine*, vol.49, no. 5, pp.838-847, 2003

[8] H.-Y. Lai, J. R. Younce, D. L. Albaugh, Y.-C. J. Kao, and Y.-Y. I. Shih, "Functional MRI reveals frequency-dependent responses during deep brain stimulation at the subthalamic nucleus or internal globus pallidus.", *NeuroImage*, vol. 84, pp. 11-18, 2014

[9] F. T. Ulaby, E. Michielssen, and U. Ravaioli, "Fundamentals of applied electromagnetics", Prentice Hall, 2010, ch. 7

[10] E. J. Neafsey, E. L. Bold, G. Haas, K. M. Hurley-Gius, G. Quirk, C. F. Sievert, and R. R. Terreberry, "The organization of the rat motor cortex: a microstimulation mapping study.", *Brain Research Reviews*, vol.11, no. 1, pp.77-96, 1986

[11] S. Bestmann, J. Baudewig, H. R. Siebner, J. C. Rothwell, J. Frahm, "BOLD MRI responses to repetitive TMS over human dorsal premotor cortex", NeuroImage, vol. 28, no. 1, pp 22-29, 2005

[12] J.P Lefaucheur, X Drouot, J.P Nguyen, "Interventional neurophysiology for pain control: duration of pain relief following repetitive transcranial magnetic stimulation of the motor cortex, Neurophysiologie Clinique/Clinical Neurophysiology, vol. 31, no. 4, pp. 247-252, 2001

[13] G. Paxinos, and C. Watson, "The rat brain in stereotaxic coordinates", Academic press, 2006.